

What is the Transfer Mechanism of Photoexcited Charge Carriers for g-C₃N₄/TiO₂ Heterojunction Photocatalysts? Verification of Relative p-n Junction Theory

Nannan Yuan, Jinfeng Zhang, Sujuan Zhang*, Gaoli Chen, Sugang Meng, You Fan, Xiuzhen Zheng, Shifu Chen*

Key Lab of Clean Energy and Green Circulation, Huaibei Normal University, Anhui Huaibei, 235000, People's Republic of China

*Corresponding Authors, Tel: +86-561-3802061, Fax: +86-561-3802061. E-mail: zhangsujuanagl@163.com, chshifu@chnu.edu.cn.

Experimental materials

Titanium dioxide (TiO₂) was supplied by Aladdin Chemistry Co. Ltd and used as received. Melamine (C₃H₆N₆), rhodamine B (RhB), methylorange (MO) and bisphenol A (BPA), and other chemicals used in the experiments were purchased from China chemical reagent Ltd. 5, 5-dimethyl-1-pyrroline-N-oxide (DMPO) was obtained from Sigma Co. They are of analytically pure grade and used without further purification. Deionized water was used throughout this study.

Materials Characterization

X-ray diffraction (XRD) patterns of the prepared photocatalysts were detected by a Bruker D8 X-ray powder diffractometer using Cu K α radiation at room temperature. UV-visible diffuse reflection spectra (UV-Vis DRS) were conducted on a TU-1950 Vis-NIR spectrophotometer (TU-1950, Persee) with BaSO₄ as a reference. Field emission scanning electron microscopy (FESEM) images were studied on a FEI Quanta 650 scanning electron microscope. The morphologies and microstructures of the photocatalysts were determined by transmission electron microscopy (TEM, FEI Tecnai G2 F20) and high-resolution transmission electron microscopy (HRTEM) at an accelerating voltage of 200 kV, elemental mappings were performed using an energy-dispersive X-ray spectrometer (EDS) attached to the TEM instrument. X-ray

photoelectron spectroscopy (XPS) analysis was obtained on an ESCALAB 250 photoelectron spectrometer (Thermo Fisher Scientific) equipped with an Al Ka X-ray beam (1486.6 eV). The binding energies were corrected with reference to the C 1s peak of the surface adventitious carbon at 284.6 eV. The Brunauer-Emmett-Teller (BET) data of the samples was obtained by N₂ adsorption-desorption at 77.3 K using a Micromeritics ASAP 2460 instrument. Photoluminescence (PL) emission spectra were recorded on a JASCO FP-6500 type fluorescence spectrophotometer and time-resolved photoluminescence spectroscopy (TR-PL) was recorded on a Edinburgh FS5 fluorescence spectrophotometer.

Photocatalytic degradation

Experiments of testing photocatalytic activity were carried out in a photoreaction apparatus. The photoreaction apparatus consists of two parts. The first part is a circular quartz tube. A 375 W medium pressure mercury lamp with a maximum excitation wavelength of 365 nm is used as UV light source. The lamp is placed in a circular hollow chamber, and the water passes through the annular casing. As the water continues to cool, the temperature of reaction solution is kept at about 30 °C. The second part is a 250 mL unsealed beaker with a diameter of about 12 cm. Photocatalytic activities of the samples were evaluated by degradation of RhB, MO and BPA under the UV light. Before each experiment, the reaction suspension solution containing 0.1 g photocatalyst and 100 mL 20 ppm RhB (or 15 ppm MO or 10 ppm BPA) was stirred in the dark for 30 min to reached sorption-desorption equilibrium between the photocatalyst and the solution. At irradiation time intervals of 20 min, 15min and 10 min for the MO, RhB and BPA solution, respectively, about 5mL of the suspension was taken out and then centrifuged to remove the photocatalyst particles. Subsequently, the absorbance spectra of RhB (or MO or BPA) solutions were analyzed by a Shimadzu UV 3600 UV-vis-NIR spectrometer using deionized water as a reference sample. The photocatalytic efficiencies of RhB, MO and BPA were calculated from the following expression:

$$\text{Degradation efficiency} = (1 - C_t/C_0) \times 100\% \quad (1)$$

Where C_0 is the concentration of reactant before illumination; C_t is the concentration of reactant after illumination time t . In order to test the repeatability of the experimental results, three batches of samples were prepared. And the average values of the data were used.

Electron paramagnetic resonance (EPR) analysis

To better understand the photocatalytic reaction process, electron paramagnetic resonance (EPR) experiments using 5, 5-dimethyl-1-pyrroline N-oxide (DMPO) as a spin-trap reagent with 10 mg catalyst under visible light irradiation ($\lambda \geq 420$ nm) have been applied to detect reaction intermediates (DMPO- $\bullet O_2^-$ and DMPO- $\bullet OH$). EPR spectra were measured on an EPR spectrometer (A300, Bruker, Germany). The results confirm the formation of $\bullet OH$ and $\bullet O_2^-$ in aqueous suspensions of the samples.

Active species trapping experiments

In addition, capturing experiments of active species for RhB photodegradation adding with g- C_3N_4 , TiO_2 and g- C_3N_4/TiO_2 samples are performed to further discuss the transfer pathway of photoexcited charge. The scavengers 1,4-benzoquinone (BQ), ammonium oxalate (AO), isopropyl alcohol (IPA) and phenixin (CCl_4) are applied to capture $\bullet O_2^-$, h^+ , $\bullet OH$ and e^- , respectively.

Photoelectrical characterization

NBT- $\bullet O_2^-$ and TA- $\bullet OH$ analysis

NBT- $\bullet O_2^-$: Nitroblue tetrazolium (NBT, 2.5×10^{-5} mol/L, exhibiting an absorption maximum at 259 nm) was used to check whether there is $\bullet O_2^-$ generated in the g- C_3N_4/TiO_2 photocatalytic system. NBT can be specifically reduced by photogenerated $\bullet O_2^-$, forming the insoluble purple formazan forms in the aqueous solutions. The production of $\bullet O_2^-$ was quantitatively analysed by detecting the decrease of the concentration of NBT in the supernatant solutions with UV-vis spectrophotometer. The procedure was similar to the degradation of MO except that the solutions were replaced by 100 mL 2.5×10^{-5} M NBT under irradiation for 5 min.

TA- $\bullet OH$: Hydroxyl radicals ($\bullet OH$) generated on the surface of different photocatalysts are detected by the fluorescence spectrometer with a 5×10^{-4} mol/L basic solution of terephthalic acid (TA) mixed solution containing 2×10^{-3} M NaOH.

TA readily reacts with $\bullet\text{OH}$ to produce a highly fluorescent product (2-hydroxyterephthalic acid), whose PL peak intensity is in proportion to the amount of $\bullet\text{OH}$ radicals formed in water. The amount of TA- $\bullet\text{OH}$ adducts were recorded on a JASCO FP-6500 type fluorescence spectrophotometer.

Photocurrent and electrochemical impedance spectroscopy tests

The photoelectrochemical tests were carried out on a three-electrode system (CHI-660E, Chenhua Instruments Co., China). A Pt wire and Ag/AgCl were used as counter electrode and reference electrode, respectively. The sample powder was deposited on the fluoride tin oxide (FTO) substrate to serve as working electrode. The electrodes were prepared as following. The 5 mg sample was dispersed in 400 μL of deionized water. Then, the 20 μL slurry was deposited as a film on a 0.5 cm \times 0.5 cm FTO substrate. After being dried at room temperature, the working electrode was obtained.

Moreover, on the CHI 660E electrochemical workstation at a bias of 0.1 V (vs. SCE) in a standard three-electrode cell, the photocurrent response of the prepared samples were detected in a 0.2 M Na_2SO_4 aqueous solution and an intermittent on-off irradiation cycle is 20 s. EIS Nyquist plots of the samples was detected in 0.1 M KCl solution containing 0.1 M $\text{K}_3[\text{Fe}(\text{CN})_6]/\text{K}_4[\text{Fe}(\text{CN})_6]$ (1:1). The aforementioned 375 W Xe lamp ($\lambda > 400$ nm) was used as the light source.

Photogenerated charge behavior (TS-SPV)

Transient-state surface photovoltage (TS-SPV) measurements was applied to study the kinetic features of the photogenerated charges with a 355 nm laser pulse and power of 50 $\mu\text{J}/\text{pulse}$ from a third-harmonic Nd:YAG laser (Polaris II, New Wave Research, Inc.).^{1,2} These kinetic features are helpful for us to understand the mechanism of semiconductor photocatalytic reaction and have certain guiding significance for the design of outstanding photocatalysts. Practically speaking, the time-resolved-based transient-state surface photovoltage system (TS-SPV) is composed of a laser (Q-smart 450, New Wave Research, Inc.), a preamplifier with a light chopper, a photovoltaic sample cell and a 500 MHz digital phosphor oscilloscope (MC-TPV 355, Tektronix). The structure of the

transient-photovoltage-spectra sample cell is ordered ITO-mica-sample (Fig. S4, inset). TS-SPV measurements were carried out at room temperature in air atmosphere.

DFT computational calculation details

First principle DFT calculations were implemented by CASTEP module of Materials Studio software. The Perdew-Burke-Ernzerh of form exchange-correlation functional was adopted within the generalized gradient approximation. A cut-off energy of 320 eV and the Monkhorst Pack k-mesh of $3 \times 3 \times 1$ for anatase TiO_2 (001) surfaces, $3 \times 3 \times 1$ for anatase TiO_2 (101) surfaces and $2 \times 3 \times 1$ for g- C_3N_4 (001) surfaces were employed. The convergence criteria of geometry optimization were set to 5.0×10^{-6} eV per atom for energy, 0.01 eV per Å for maximum force, 0.02 GPa for maximum pressure and 5.0×10^{-4} Å for maximum displacement.

E_{VB} and E_{CB} calculation of g- C_3N_4 and TiO_2

According to the following empirical equation, the band edge positions of the CB and VB of g- C_3N_4 and TiO_2 can be determined by the following equation:

$$E_{\text{VB}} = X - E_e + 0.5 E_g$$

$$E_{\text{CB}} = E_{\text{VB}} - E_g$$

Where E_{VB} , X , E_e and E_{CB} are the VB edge, the absolute electronegativity of the semiconductor, the energy of free electrons on the hydrogen scale (likely 4.5 eV) and the CB potential, respectively. The X values for g- C_3N_4 and TiO_2 are 4.73 and 5.81 eV, respectively. From the calculation, the E_{CB} of g- C_3N_4 and TiO_2 are -1.13 and -0.32 eV, and the E_{VB} of g- C_3N_4 and TiO_2 are estimated to be 1.58 and 2.94 eV, respectively. It agrees well with the previous reports.^{3,4}

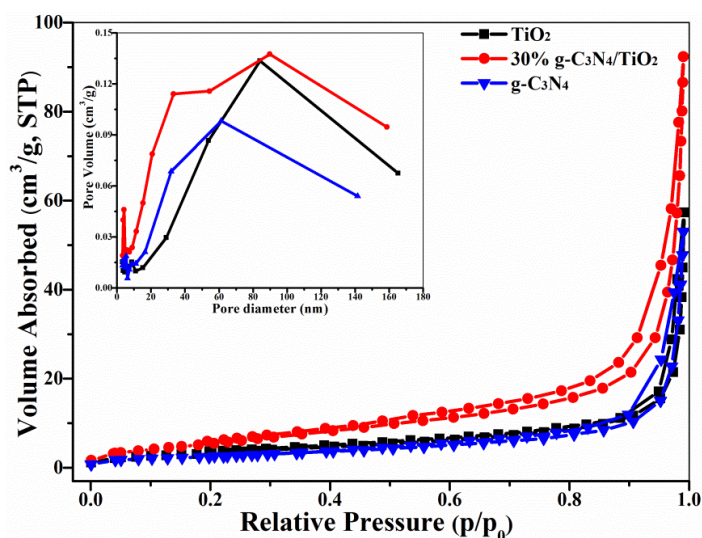


Figure S1. Nitrogen adsorption-desorption isotherms and the corresponding pore-size distribution curves (inset) of the g-C₃N₄, TiO₂ and g-C₃N₄/TiO₂ samples.

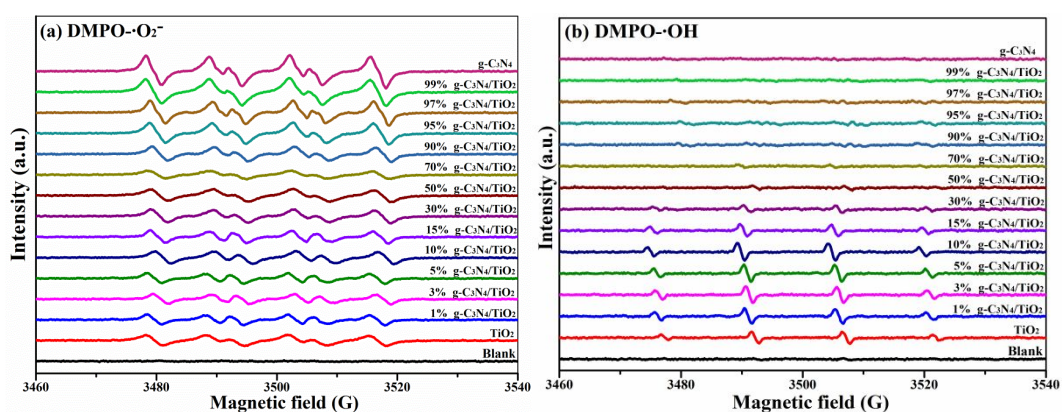


Figure S2. EPR signals of (a) DMPO-•O₂⁻ adduct and (b) DMPO-•OH adduct over different samples under UV-light irradiation for 60 s in methanol and aqueous dispersion, respectively.

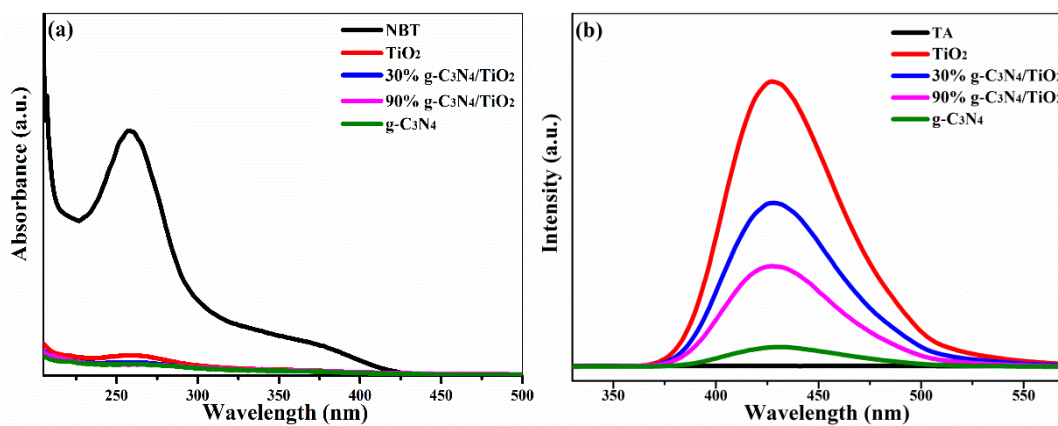


Figure S3. (a) The absorbance of the NBT solution contained no photocatalyst (blank), TiO₂, g-C₃N₄ and g-C₃N₄/TiO₂ heterojunctions for detecting •O₂⁻. (b)

Photoluminescence (PL) emission spectra of the TA-•OH adduct formed under UV-light irradiation for different samples in TA solution.

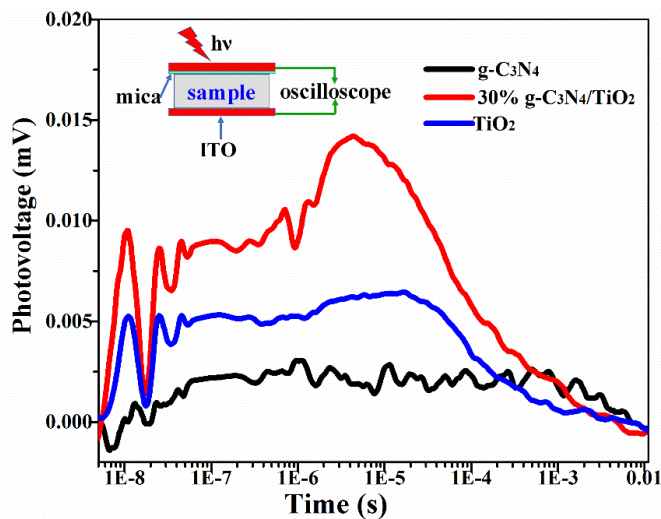


Figure S4. TS-SPV responses of TiO_2 , $\text{g-C}_3\text{N}_4$ and $\text{g-C}_3\text{N}_4/\text{TiO}_2$ samples under a 355 nm laser pulse and power of $50 \mu\text{J/pulse}$. Insets show the schematic setup of TS-SPV measurement.

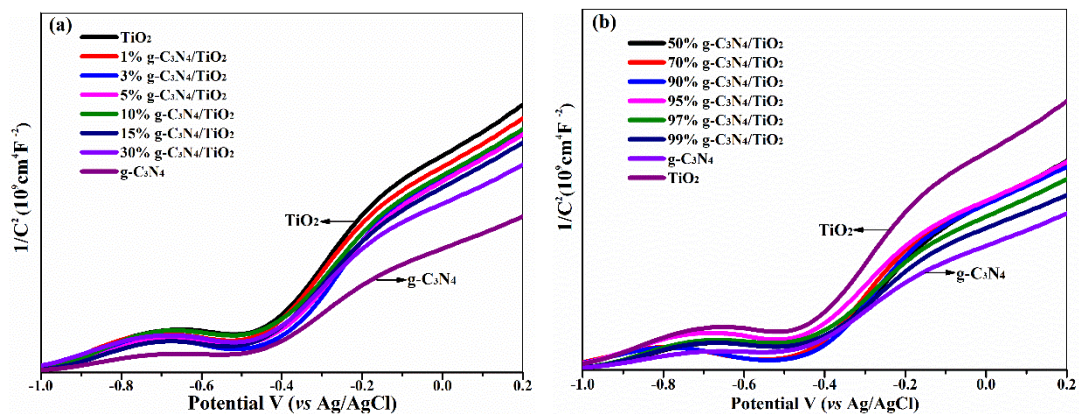


Figure S5. Mott-Schottky plots of the samples.

| Sample | Slope |
|--|--------|
| TiO_2 | 6.85E9 |
| 1% $\text{g-C}_3\text{N}_4/\text{TiO}_2$ | 6.54E9 |
| 3% $\text{g-C}_3\text{N}_4/\text{TiO}_2$ | 6.28E9 |

| | |
|---|--------|
| 5% g-C ₃ N ₄ /TiO ₂ | 6.27E9 |
| 10% g-C ₃ N ₄ /TiO ₂ | 6.26E9 |
| 15% g-C ₃ N ₄ /TiO ₂ | 6.07E9 |
| 30% g-C ₃ N ₄ /TiO ₂ | 5.24E9 |
| 50% g-C ₃ N ₄ /TiO ₂ | 5.55E9 |
| 70% g-C ₃ N ₄ /TiO ₂ | 5.38E9 |
| 90% g-C ₃ N ₄ /TiO ₂ | 5.33E9 |
| 95% g-C ₃ N ₄ /TiO ₂ | 5.24E9 |
| 97% g-C ₃ N ₄ /TiO ₂ | 4.96E9 |
| 99% g-C ₃ N ₄ /TiO ₂ | 4.55E9 |
| g-C ₃ N ₄ | 4.16E9 |

Table S1. The linear slopes of the Mott-Schottky plots for the samples.

References

- (1) Wei, X.; Xie, T. F.; Xu, D.; Zhao, Q. D.; Pang, S.; Wang, D. J. A Study of the Dynamic Properties of Photo-Induced Charge Carriers at Nanoporous TiO₂/Conductive Substrate Interfaces by the Transient Photovoltage Technique. *Nanotechnology* **2008**, *19*, 275707.
- (2) Jiang, T. F.; Xie, T. F.; Chen, L. P.; Fu, Z. W.; Wang, D. J. Carrier Concentration-Dependent Electron Transfer in Cu₂O/ZnO Nanorod Arrays and their Photocatalytic Performance. *Nanoscale* **2013**, *5*, 2938-2944.
- (3) Hao, R. R.; Wang, G. H.; Jiang, C. J.; Tang, H.; Xu, Q. C. In Situ Hydrothermal Synthesis of g-C₃N₄/TiO₂ Heterojunction Photocatalysts with High Specific Surface Area for Rhodamine B Degradation. *Appl. Surf. Sci.* **2017**, *411*, 400-410.
- (4) Chen, S. F.; Hu, Y. F.; Meng, S. G.; Fu, X. L. Study on the Separation Mechanisms of Photogenerated Electrons and Holes for Composite Photocatalysts g-C₃N₄-WO₃. *Appl. Catal. B: Environ.* **2014**, *150-151*, 564-573.